Int. J. Industrial. Model. chem. 2025; 16(2) 1-11

International Journal of Industrial Chemistry (IJIC)

https://doi.org/10.57647/j.ijic.2025.1602.10

Green Synthesis and Investigation of the Functional Behavior of Carbon Quantum Dots in Elastomeric Compounds Based on (BR/SBR)

Mohamadamin Vosooghnia, Fereshteh Motiee*, Arman Van

Department of Chemistry, North Tehran Branch, Islamic Azad University, Tehran, Iran

***Corresponding author:** f_motiee@iau-tnb.ac.ir

Original Research

Received:
10 March 2025

Revised:
13 May 2025

Accepted:
28 May 2025

Published in Issue:
30 June 2026

Abstract

In this study, carbon quantum dot nanomaterials obtained from sugarcane bagasse have been used in the liquid phase in five distinct formulations as a substitute for aromatic oil and part of carbon black in BR/SBR elastomeric compounds. This research aimed to study the rheological, mechanical, and thermal properties of the compounds developed with carbon quantum dots. DLS (Dynamic Light Scattering), HR-TEM (High-Resolution Transmission Electron Microscope), FESEM (Field Emission Scanning Electron Microscope), and FTIR (Fourier Transform Infrared Spectroscopy) were used to characterize the carbon quantum dot. Also, tensile strength, wear, rheometry, and Thermogravimetric analysis (TGA) tests were used to check elastomeric compounds' mechanical, rheological, and thermal properties. Based on the obtained data, sample N3 showed the best rheological, mechanical, and thermal properties among the manufactured samples. Overall, these nanomaterials are expected to be an appropriate substitute for the aromatic oil used in the rubber industry

Keywords: BR/SBR elastomeric compounds, Carbon quantum dot, FESEM, HR-TEM, Mechanical analysis, Sugarcane bagasse

Cite this article: Vosooghnia M., Motiee F., Van A. (2025). Green Synthesis and Investigation of the Functional Behavior of Carbon Quantum Dots in Elastomeric Compounds Based on (BR/SBR, *International Journal of Industrial Chemistry*, 16(2)*:* 1-11. https://doi.org/10.57647/10.57647/j.ijic.2025.1602.10

1. Introduction

Rubbers are considered an "elastomer" in classifying polymers that can swiftly recover from deformation [1]. These materials have appropriate mechanical properties. However, in the raw state, they have defects such as low resistance to organic solvents and low thermal resistance. As a result, they require chemical reforms, such as using additives or combinations with other polymers [2]. The invention of vulcanization technology and the use of additives by Goodyear and Hancock in 1839 further expanded its utilization and efficiency [3]. In fact, During this process, the long chain molecules crosslinking with high molecular weight transforms them from thermoplastic (visco-elastic) and sticky to thermoset (elasto-viscous) and resistant to high heat with favorable mechanical and chemical properties. Therefore, the vulcanization process aims to obtain elastomers with high mechanical properties that can be used in various industries [4]. In previous studies, scientists have evaluated various rubbers, which can be mentioned NR (Natural Rubber), SBR (Styrene-Butadiene Rubber), BR (Polybutadiene Rubber), IIR (Isobutylene Isoprene Rubber), and SBS (Polystyrene-Butadiene-Styrene) [5]. Generally, to obtain novel polymer composite materials with industrial applications and desirable mechanical properties, mixing two or more elastomers can be used [6]. The

connection of two or more suitable properties of single vulcanized elastomers in a material can be an apparent reason for preparing a combination of two elastomers [7]. Styrene-butadiene elastomer (SBR) is a copolymer composed of styrene and butadiene monomers [8]. In addition, it performs more prominently in wear, thermal aging, water resistance, and gas penetration compared to Natural Rubber (NR) [9] .

On the other hand, cis-polybutadiene (BR) does not exhibit high tensile strength and is usually blended with another elastomer [10]. However, cis-polybutadiene (BR) elastomers display higher wear and low rolling resistance than SBR and NR. That is why polybutadiene (BR) is combined with SBR or NR to make rubber treads [11].

Despite all the advantages mentioned, rubber without additives, in most cases, even after the vulcanization process, cannot meet the basic needs of the industry [12]. One of the critical additives is fillers. Fillers are particles added to tires to improve surface characteristics and dimensional stability and change thermal and mechanical properties [8]. Essential parameters such as particle geometry and dimensions, volume fraction, dispersion quality, and interaction between fillers and rubber affect their properties and processability. Therefore, the intelligent selection of consumable fillers in a particular polymer matrix and the optimization of appropriate processing methods require careful study and evaluation [13]. However, the most commonly used commercial reinforcing fillers are carbon black (CB) and silica [14]. Commonly, carbon black is made from incomplete heavy petroleum products combustion, including ethylene cracking tar, coal tar, FCC tar, and some vegetable oils [15]. Despite its remarkable reinforcing properties, carbon black is a non-renewable resource derived from petroleum. From the point of view of green and sustainable chemistry, the current situation of carbon black is firmly under observation, and much research has been conducted to obtain new alternatives with low pollution of the environment and similar performance to enhance rubber properties [16,17]. Nanofillers are one of these alternatives. They can be distributed as separate particles within the polymer matrix, with at least one dimension at the nanoscale. This leads to the creation of a polymer matrix that exhibits a high degree of reactivity. The small size of the constituent particles and the enhancement in the surface interaction area can be vital reasons for the presence of nanofillers in the matrix of rubber, which improves the polymer properties with low filler loading. The particle size, morphology, and filler surface activity are critical parameters in controlling the reinforcing impact on rubbers. Today, innovative research focuses on carbon-based nanofillers [18,19] .

Carbon quantum dots (CQD) are a novel group of semiconducting carbon nanomaterials with particle sizes < 10 nm [20]. Due to the smallness of the particles and their three-dimensional placement in the nanoscale, this group of materials is also considered as zero-dimensional (0D) nanomaterials [21]. Regarding their shape, they possess spherical symmetry and exhibit an intermediate structure between crystalline and amorphous. Both structures can display impressive characteristics, including light emission that varies with wavelength, ease of functionalization, low toxicity, high solubility, and biocompatibility [22]. According to recent studies, small amounts of these nanomaterials do not exhibit significant toxicity to cells, and it has even been reported that, in some cases, they can enhance the growth of living cells [23]. Furthermore, due to the widespread application of carbon quantum dots, their green synthesis is of interest. The use of agricultural waste has been highly appreciated due to its low cost, wide availability, and environmental friendliness [24]. Carbon quantum dots can have functional groups on their surface. The most common functional groups are amino groups (–NH2), carbonyl groups (–CO), carboxyl groups (–COOH), and hydroxyl groups (–OH) [25]. In terms of applications, all these superior properties have made CQDs well-used in sensing, biomedicine, electrochemical reactions, bioimaging, photocatalysis, and drug delivery [26,27]. Carbon quantum dots can be produced in two comprehensive ways. In top-down approaches, large carbon precursors are broken into nano-size. In contrast, the bottom-up approach includes putting atoms together to develop nanoparticles [28,29]. This research aimed to use a carbon quantum dot solution synthesized from sugarcane pulp as a substitute for standard aromatic oil in the rubber industry and a part of carbon black in elastomeric BR/SBR compounds, which had not been used until now. Further, the role and effect of carbon quantum dot samples in improving mechanical properties and reducing harmful environmental effects have also been evaluated.

2. Materials and methods

2.1. Materials

Sugarcane Bagasse purchased from (Ahvaz, Iran) was utilized to prepare carbon quantum dots. Toluene (≥ 99.9%), produced by (Merck, Germany) was used as the solvent of the CQD system. SBR 1500 (1502) and BR 01, manufactured by (THE AHAU (GM) Company, Malaysia) were utilized as the investigated elastomers. Furthermore, Mixing agents include Carbon Black (N-339) manufactured by (Pars et al. Company, Iran), Aromatic oil 250 made by (Iranol company, Iran),

Stearic Acid made by (klk company, Malaysia), Zinc Oxide (ZnO) made by (Shokohieh company, Iran), Anti-ozone (4020-40106) IPPD made by (Stair Chemical, China), TMQ accelerator made by (HENAN company, China), Ordinary sulfur for Vulcanization made by (Iran's Tsedak Company, Iran), CZ accelerator made by (MOI Company, China), DPG accelerator made by (RICHON Company, China) and paraffin wax made by (Iran Shimi Company, Iran) were purchased.

2.2. Methods

2.2.1. *Carbon Quantum Dot (CQD) Preparation*

Carbon quantum dots were produced by altering the method described by Thambiraj et al. in 2016 [30]. We put a certain amount of dry sugarcane pulp (bagasse) inside the electric furnace for 30 minutes and set its temperature to 300°C. Then we weighed 1 gram of semi-carbonized bagasse, poured it into a 250 ml beaker, and added 100 ml of toluene. In the next step, the obtained mixture is placed on the heater stirrer for 24 hours until it becomes a single phase. Then, we put the material obtained in the ultrasonic device and immediately put it in the centrifuge for 45 minutes at 9000 revolutions. In the last step, we collected the supernatant from the centrifuge for further tests and characterization.

2.2.2. Manufacturing of Rubber Nanocomposites

In this section, six different formulations, including the blank sample, were developed at room temperature with a relative humidity of 45%. The difference between the samples is the amount of CB and the presence or absence of paraffin wax. Also, the carbon quantum dot solution was not used as aromatic oil in the blank sample, and the standard aromatic oil in the industry was used. Carbon quantum dot solution was entered into the mixture formulation as a substitute for aromatic oil. Also, the amount of carbon black was changed according to the mentioned formulations in different samples. This process investigated an elastomeric mixture's mechanical, chemical, and thermal properties based on BR/ SBR in the presence of carbon quantum dots.
The samples were made using a double roller mill in two steps. First, the elastomeric mixture was prepared along with the filler, and then, in the next step, curing agents were added to it. The roller's and the mixture's temperature were controlled during the mixing process. The order and approximate time of mixing is as follows:
1) Softening and mastication of the elastomeric mixture for about 15 minutes
2) Adding fillers to the mixture for about 10 minutes
3) Adding powdered ingredients in about 5 minutes
4) Adding curing agents in about 5 minutes
After mixing, the mixtures rested for 24 hours at controlled temperature and humidity. Then, the rheological and thermal properties of the mixtures were investigated. Moreover, it was finally tested for other analyses.

2.3. Characterization studies

This section is divided into two distinct parts. Initially, the characterization of carbon quantum dots obtained from sugarcane pulp was investigated. In the next stage, the characterization of rubber samples developed by carbon quantum dots was evaluated.

2.3.1. *Characterization of carbon quantum dot*

Multiple spectroscopic and optical methods characterized the synthesized carbon quantum dots.

2.3.1.1. *FESEM (Field Emission scanning electron microscope)*

Surface images and morphology of carbon quantum dot samples were prepared using a FESEM through the Zeiss-ƐIGMA300 instrument. The main benefit of analysis FESEM compared to analysis (SEM) is its far better resolution due to the field emission electron production source. A portion of the sample that was dried by the freeze-drying method was placed inside the gold coating and analyzed. The sample components were also analyzed using this instrument's EDS (energy-dispersive X-ray spectroscopy) detector at an accelerating 25 kV voltage.

2.3.1.2. *HR-TEM (High-resolution transmission electron microscope)*

More detailed morphology, particle size, and dispersion level of the carbon quantum dot sample were investigated using HR-TEM through the FEI- Tecnai F20 instrument. For imaging, a few drops of CQD solution were poured on a grid with carbon coating; the sample was prepared for imaging after the solution dried on the grid. In addition, the average particle size histogram image was prepared using the same instrument.

2.3.1.3. *DLS (Dynamic Light Scattering)*

DLS is an effective method for evaluating nanoparticles and assessing their characteristics in a liquid medium [31]. Unlike microscopic methods, this technique can assess particles' size or distribution when suspended in a

liquid. It relies on the variations in the severity of visible light scattered by particles as they move randomly due to Brownian motion in the liquid. 10 ml of CQD solution was used to analyze and measure nanoparticles using a Scatteroscope- Qudix instrument.

2.3.1.4. *FT-IR (Fourier Transform Infrared) Spectroscopy*

FT-IR spectroscopy identified the surface functional groups. The FT-IR spectrum was captured with a Bruker Tensor II spectrometer, spanning the spectral range of 650–4000 cm−1 at room temperature [30].

2.3.2. *Characterization of elastomer compounds*

Multiple mechanical, rheological, and thermal tests assessed the manufactured rubber nanocomposites.

2.3.2.1. *Rheometry test*

A rheometer was used to determine the curing state. This instrument (MDR-HIWA 900) has a conical disc and an oscillating motion instead of a rotary one. This instrument gave us a graph showing the time's horizontal axis and the torque's vertical axis. This test follows the ASTM D 5289 standard. Also, the maximum torque (MH), minimum torque (ML), optimum curing time (TS2), middle curing time (TC50), and curing time (Tc90) can be extracted from this test.

2.3.2.2. *TGA (Thermogravimetric Analysis)*

TGA is a commonly utilized method for thermal evaluation. This method involves assessing the mass loss of materials to temperature changes. During thermal analysis, a continuous graph shows mass versus temperature when a sample is heated at a consistent rate or maintained at a steady temperature. The resulting graph, known as a thermogravimetric (TG) curve, typically displays mass (m) decreasing on the y-axis while temperature (T) increases along the x-axis. This analysis was conducted using a TGA model Q600 instrument from TA Company in the United States, capable of operating within a temperature range of 25 to 800 °C at a 10 °C/min rate on uncured samples. Inert gas (argon) atmosphere was used from 25 to 400°C, and air atmosphere from 400 to 800°C.

2.3.2.3. *Tensile strength test*

This test is one of the most important mechanical tests performed after curing. The tensile test begins by shaping a flat rubber sheet approximately 2 mm thick, from which dumbbell-shaped samples are cut out. These samples are then subjected to stretching in a tensile testing machine, where the force necessary to extend them to the point of fracture is recorded. Stress values, calculated by dividing the force by the original cross-sectional area of the straight section of the dumbbell, are documented at various extension levels until the breaking point.

The amount of expansion of the sample is measured as a percentage of the increase in length and is defined as follows:

$$\frac{L - Lo}{Lo} \times 100$$

Tensile values before breaking the sample indicate the Modulus of the sample. To a rubber specialist, Modulus means the amount of stretch (stress) at a given elongation. In other words, Modulus numbers are usually measured in elongation of 100%, 200%, and 300%. Another is the ratio of stress to strain. Another important function of tensile testing is to determine the dispersion of materials in the rubber compound during the mixing stage. This test was done by (A universal-M350-5KN) tension instrument with 500 mm.min-1 speed that follows the ASTM D412 standard.

2.3.2.4. *Wear test*

The gradual loss of the surface of a tire in contact with a rough surface is called wear. The basis of all wear tests is the relative motion between the rubber and a rough surface under a constant force. The most common method of determining wear is measuring the weight loss percentage after the test per mm [3] . In this way, first, the weight of the sample is determined before performing the test, and then after performing the wear test, the secondary weight of the sample is measured. The amount of wear is obtained by dividing the difference between secondary and primary weight by primary weight.

$$\frac{W0 - W1}{W0} \times 100$$

This test was performed according to ISO 4649 (10 N load, 0.3 m/s, SiC abrasive, 40 m sliding distance) using the AB602103 Abrasion Testing Machine from Bareiss Company in Germany.

2.3.2.5. *FESEM*

To control the interaction and dispersion of the components of the rubber compound, a FESEM was used.

a)

b)

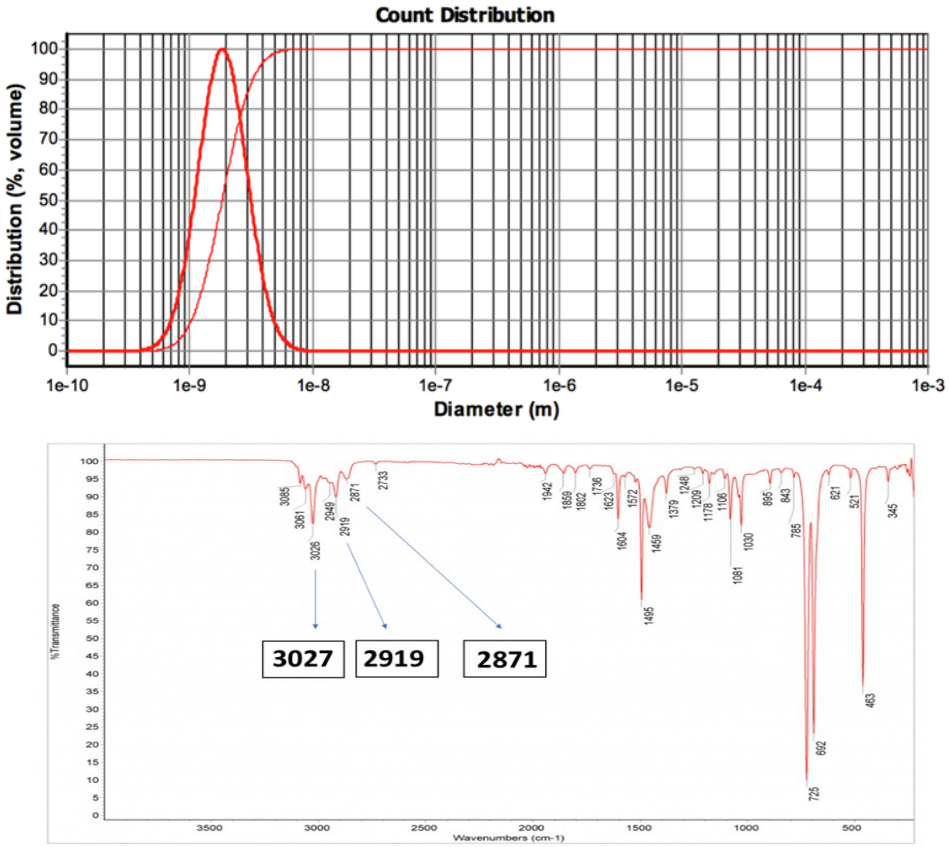

Figure 1. a) DLS analysis of CQDs, indicating an average size of 1.84 nm, **b)** FT-IR spectrum of synthesized CQDs

3. Results and discussion

3.1. Carbon quantum dot characterization

3.1.1. *DLS (Dynamic Light Scattering)*

The results of DLS analysis are influenced by the interaction of incident laser light with spherical particles in the analyte that exhibit natural Brownian motion. Scattered light is emitted in various directions and possesses different wavelengths and intensities over time. Consequently, the intensity of light scattering from nanoparticles is proportional to the sixth power of the particle radius. Thus, the diffusion coefficient obtained through DLS reflects the equivalent hydrodynamic size [32]. According to the findings of the DLS test in the conducted research, the average particle size is 1.84 nm, which can be seen in the peak obtained from Figure 1a. In this graph, the horizontal axis reveals the size of the sample particles based on meters, and the vertical axis demonstrates the distribution percentage of the sample particles. As mentioned earlier, carbon dots are nanoparticles smaller than 10 nm [33]. So, in terms of the size of the particles, it can be predicted that this sample is a quantum dot.

3.1.2. *FT-IR spectroscopy*

Based on the peaks of this spectrum in Figure 1b, it shows strong absorption bands at (2919 cm-1) and (2871 cm-1), which are related to the C=C stretching vibration of methylene or methyl groups present in CQD with toluene. Indeed, another weak absorption peak at (3085 cm-1) can be related to the presence of hydrogen bonds, which indicates the presence of O-H functional groups on the carbon quantum dot surface. Also, an absorption band can be seen at the point (1736 cm-1), which is related to the carbonyl group C=O 30. Additionally, the peak at 1604 cm−1 confirms the presence of an aromatic C=C bond [34].

3.1.3. *FESEM*

This test determines the morphology and shape of the particles, but no accurate information is obtained regarding the size of the particles [35]. Also, EDS is obtained via this test, which determines the percentage and type of elements in the sample. From the images in Figures 2a and 2b, it can be concluded that the shape of carbon quantum dot particles is spherical, and the amount of dispersion is appropriate. Also, from the EDS data in Figure 1c, it can be found that 80% of the carbon quantum dot sample contains carbon and 20% oxygen

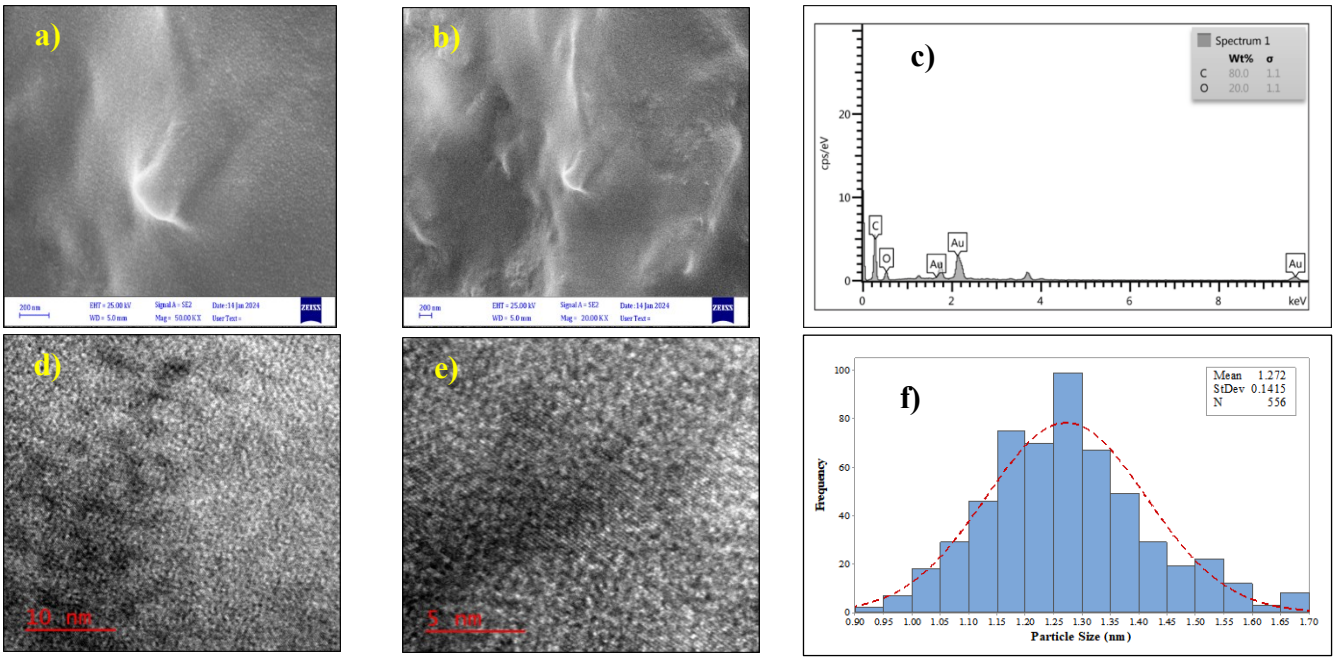

Figure 2. FESEM Images of CQDs. **a)** High magnification image, **b)** Low magnification image, **c)** EDS image of CQDs, indicating the 80% of pure carbon and 20% of oxygen, HR-TEM Images of CQDs. **d)** At 10 nm scale, **e)** At 5 nm scale, **f)** Histogram image of CQDs with an average size of 1.272 ± 0.14 nm between 556 particles corresponding to the image of (e)

(This is probably due to oxygen related to functional groups). This is almost the same as other research 30.

3.1.4. *HR-TEM*

This analysis was utilized to accurately check the particle size of the carbon quantum dot sample [36]. In a similar study, HR-TEM images clearly show that CQDs are very small, almost spherical, and single-phase, and the obtained carbon quantum dots have a graphite-like structure [30]. Based on the images obtained from the transmission electron microscope in Figures 2d and 2e, the carbon quantum dot sample particles have an acceptable dispersion and are almost spherical [37]. Moreover, based on the average particle size histogram results, the particle size range is between 1 and 2 nm. In addition, the average particle size among 556 particles is approximately 1.27 nm.

3.2. Rheological attributes of rubber compounds

3.2.1. *The amount of torque at the minimum and maximum points (ML, MH)*

One of the investigated parameters of the curing behavior of rubber compounds was the difference of torques at the minimum and maximum point, which is indirectly associated with the density of the crosslinks formed during curing. In general, the higher this value is, the higher the density of crosslinks. The maximum moment (MH) measures the hardness and shear modulus of the wholly cured composite at the temperature of curing, and the strong interaction between the filler and the polymer chains enhances the maximum torque. Data related to torques are given in Table 2 for the blank sample and five manufactured samples. As mentioned in Section 1, the vulcanization process, which involves the addition of sulfur or peroxides along with curing agents (depending on the elastomer type), is essential to obtain usable and durable elastomers. Throughout this process, the creation of crosslinks converts long-chain molecules from a soft plastic material into a more robust elastomer that exhibits high resistance to aging and heat. As a result, crosslink density is a crucial factor that influences the ultimate properties of elastomeric compounds.
On the other hand, in common, the carbon nanofillers addition that is more rigid than the soft rubber matrix increases the crosslink density of the rubber chains, and it has been mentioned that with the increase of nanofillers (carbon quantum dots), the torque values at the maximum point increase [38,39]. Based on the data in Table 2, the torque difference in the quintuple data is more significant than the blank sample, indicating an enhancement in the density of crosslinks connections compared to the commercial blank sample. According to the explanations, although carbon quantum dots have not been used in the rubber industry, their presence as a zero-dimensional nanofiller, instead of aromatic oil and part of carbon black, could be the reason for this increase.

3.2.2. *Optimum curing time (Ts2) and curing time in 90% mode (Tc90)*

The following parameters that were assessed were

optimal curing time and curing time. The optimal curing or scorching time is when the torque is two units more than the minimum. Also, the curing time, which represents the time for forming 90% of crosslinks in rubber compounds that have an inverse relationship with the curing rate, was measured. Adding nanoparticles in optimal curing time and curing time of the prepared all dispersion procedures decreases the scorching and curing time [40] . According to Table 2, as predicted, the compounds were generally reduced compared to the commercial control sample.

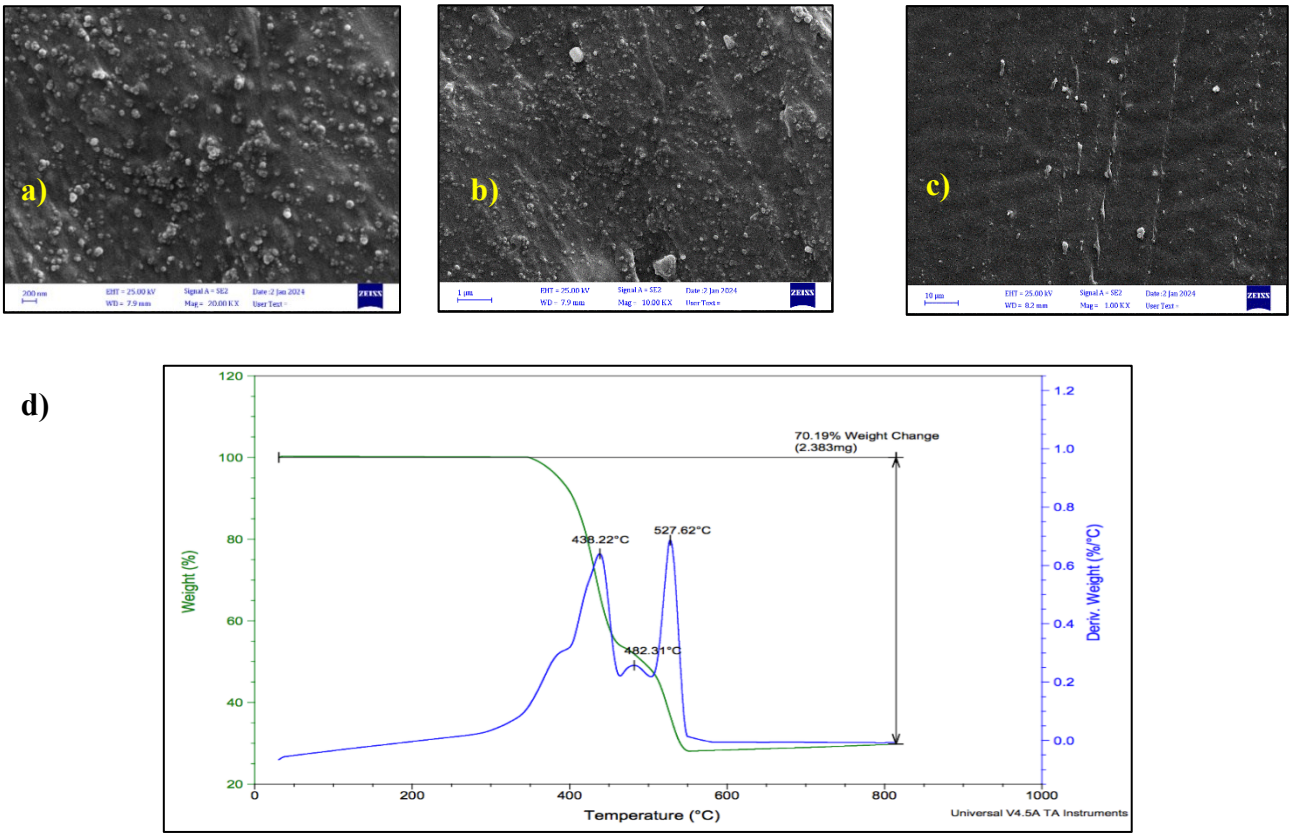

Figure 3. FESEM Images of N_3 compound. **a)** At 200 nm scale, **b)** At 1 µm, **c)** At 10 µm. **d)** TGA analysis of N_3 compound.

Table 1. Formulation of developed compounds

	Component (phr)	Blank sample	N_1	N_2	N_3	N_4	N_5
1	SBR 1500 (1502)	80	80	80	80	80	80
2	BR 01	20	20	20	20	20	20
3	Carbon Black (N-339)	50	50	45	45	40	40
4	Aromatic Oil	30	30	30	30	30	30
5	St. Acid	2	2	2	2	2	2
6	ZnO	5	5	5	5	5	5
7	IPPD(4020-40106)	1.5	1.5	1.5	1.5	1.5	1.5
8	TMQ	2	2	2	2	2	2
9	S	2	2	2	2	2	2
10	CZ	1	1	1	1	1	1
11	DPG	0.5	0.5	0.5	0.5	0.5	0.5
12	Paraffin Wax	2	2	2	0	2	0
13	phr total mass balance	196	196	191	189	186	184

Table 2. Rheological result of developed compounds

Sample	M_H (dN/m)	M_L (dN/m)	$M_H - M_L$ ΔH	CRI Min^{-1}	T_{S2} (Sec)	T_{C90} (Sec)
N_1	12.21	1.954	10.256	30.593	119	294
N_2	11.844	1.709	10.135	29.399	124	313
N_3	12.332	1.954	10.378	30.663	125	295
N_4	10.256	1.465	8.791	32.957	139	308
N_5	10.989	1.587	9.402	30.139	137	312
Blank Sample	8.8	1.91	6.89	14.05	223	650

3.2.3. *Curing Rate Index (CRI)*

This parameter determines the speed of the curing process. The curing rate indicates the speed of crosslink formation in the compound, which has an inverse relationship with curing time. The higher the curing speed, the shorter the curing time. Looking at all rheometer test parameters and curing attributes, it can be concluded that adding nanoparticles to the elastomeric mixture significantly improves the curing properties [40]. Table 2 shows the curing rate of the commercial blank sample and five other manufactured samples. As presented in the table, the curing rate index of the prepared compounds has increased significantly.

3.3. Mechanical and thermal attributes of rubber compounds

3.3.1. *Tensile strength*

At first, the tolerable stress of the compounds up to the breaking point was evaluated in terms of (MPa), which, based on Table 3, indicates the amount of tensile strength. As can be seen, the manufactured samples' tensile strength (tension) has increased compared to the blank sample used in the industry. As mentioned, based on EDS results, 80% of the carbon quantum dot sample consists of carbon. Furthermore, carbon is the main component of carbon black (CB) [41] —the nature and

performance of these two substances as fillers are expected to be similar.

On the other hand, the carbon quantum dot in this compound is a suitable substitute for aromatic oil and can be more effective in mixing the compounds. In this case, this similarity can lead to more filler-filler interaction (CB/CQD) and ultimately cause an increase in the density of crosslinks [38]. Also, according to the histogram images of the average particle size of carbon quantum dot samples, these particles are below 10 nm and are considered in 3 dimensions at the nanoscale [42]. Conversely, the rubber tensile strength can be significantly enhanced by the addition of carbon nanofillers, with the extent of improvement influenced by the filler's structure within the matrix (such as dispersion level, particle bonding, and network formation) and the interactions between the filler and rubber. Typically, incorporating carbon nanofillers into rubber leads to two main effects: it adds stiffness and strength through the filler itself and increases the compound crosslink density. The filled elastomer compound's exceptional tensile strength results from the filler network's synergistic effects, rubber-filler interactions, and the crosslinked chemical networks within the rubber matrix. So, this relative increase can be justified based on the abovementioned reasons. Sample N3 has the highest tensile strength, which is worth pondering. Based on the former research, the impact of nanofiller content on the reinforcement of filled elastomer compound follows a common rule: with the increase in the percentage of nanofiller, the tensile strength gently enhances up to a peak value. Then, it decreases with the increase in nanofiller percentage [38]. With these interpretations, it can be predicted that sample N3 has the highest density of crosslinks and the highest amount of filler-filler interaction.

3.3.2. *Elongation*

The following mechanical parameter investigated was the elongation percentage at the breakpoint. As seen in Table 3, except for the N5 sample, the relative amount of this parameter is almost equal to or more than the blank sample used in the industry of rubber. Carbon black and quantum dot fillers have been utilized in different proportions in this research operation. This enhancement can be explained by the incorporation of secondary fillers (carbon quantum dots) in composites of carbon nanofiller/rubber, which can improve the exfoliation or dispersion of carbon nanofillers or create

an optimal structure within the matrix of rubber, leading to a synergistic strengthening impact. The particles of dispersed filler help to deflect or halt the propagation of cracks, resulting in increased resistance to fracture 38. According to the research results, the interactions between two or more filler arrangements increase the dispersion of the filler and the efficient shift of stress from the matrix, which leads to the recovery of the mechanical and dynamic attributes of the compound. These combined nanocomposites generally demonstrate an enhancement in tensile strength, elongation, and Modulus compared to the blank micro-composite [43].

3.3.3. *Modulus at 100% and 300% points*

The Modulus of the compounds was another mechanical parameter that was investigated. As can be seen, the hardness of the compounds in elongation (100%) is higher than the blank sample. Generally, incorporating carbon nanofillers, which are stiffer than the matrix of soft rubber, enhances the crosslink density of the rubber chains, thereby increasing the material's elastic Modulus [38]. In addition, as previously mentioned, based on HR-TEM data analysis, the structure of carbon quantum dots is similar to graphite [30]. In past research, graphite as a filler in connection (bonding) with carbon black in rubber has improved the mechanical attributes of the elastomeric compound [44]. Additionally, the dimensions of carbon nanofillers play a significant role in influencing the overall performance of the resulting nanocomposite. A related study examined how the size of carbon nanofiller particles impacts the mechanical properties of a specific type of rubber composite, utilizing micrometer, expanded, submicrometer, and spherical graphite fillers. Development graphite showed the highest Young's Modulus (MJ) because of its smaller size than other graphites, causing better reinforcement than larger particles with less surface area [45,46].

3.3.4. *Wear*

According to the wear test data in Table 3, the amount of wear in the five compounds is lower than in the blank sample. Based on the results provided in the previous section, the general structure of carbon quantum dots is similar to graphite [30]. One research used graphite with the smallest size as a filler. As expected, this filler had the best strengthening ability. Tribological properties (tribology deals with friction, wear, and lubrication of interacting surfaces) rubber was further improved by adding graphite. Sub-micrometer (smallest particle size) graphite has provided the best wear characteristics for rubber compounds compared to other fillers. Also, the size and shape of filler particles have a pivotal effect on the tribological attributes of polymers. Nano-sized fillers have been used to simultaneously improve polymer composites' ternary and mechanical properties. In rubber reinforcement, a key characteristic of the reinforcing filler is that it should be small, allowing the filler particles to possess a large surface area for interaction with the rubber [47]. Overall, nanoparticles can enhance the strength of the interface layer and minimize the composite wear, as the fillers are comparable in size to the sections of the adjacent polymer chains [46]. ANOVA confirmed significant differences ($p < 0.05$) between formulations in all mechanical and wear data.

3.3.5 *TGA of N3 compound*

The following parameter that was investigated was the thermal behavior of the compounds. This test conducts a comprehensive investigation of the compound as a function of temperature. The rate of temperature change was ten °C/min. Also, an inert gas (argon) atmosphere was used from 25 to 400°C, and an air atmosphere was used from 400 to 800 °C. Based on previous research, the thermal stability of polymer nanocomposites is enhanced by incorporating nanofillers into the rubber matrix. The improvement in thermal properties is due to the nanofillers forming irregular pathways that prevent direct heat transfer to the degrading polymer compound and insulate the underlying polymer from thermal degradation.

Also, well-dispersed nanofillers prevent premature thermal degradation of the elastomer. Therefore, the addition of nanofillers accurately increases the initial degradation of composites and maintains the thermal stability of the samples [48 ,49]. Figure 3d is the diagram for sample N3.

As can be seen, the first degradation point based on the differential thermogravimetry (DTG) test is at 438°C. The next point is at 482°C, and the third is at 527°C. This sample was destroyed in 3 stages. Also, generally, it has had a weight change of almost 70%. According to the obtained results, it can be predicted that the formulation can be effectively used in heat-resistant rubber industries. 3.3.6. *FESEM of N3 compound*

The images of this analysis can be used to study the dispersion of filler particles in a polymer matrix [50]. Based on past research on nanofillers, the distance between particles decreases with an excessive enhancement in nanofiller loading percentage, which may lead to the accumulation of filler particles. In fact, due to the stronger-than-expected van der Waals attraction between these nanofillers, there is a tendency to aggregate within the rubber matrix [51]. According to the SEM microscope images in Figures 3a, 3b, and 3c, carbon quantum dot nanoparticles are well dispersed in the compound.

As mentioned, this sample (N3) had the highest mechanical and thermal properties among the prepared mixtures. In its formulation, 5 phr of carbon black was reduced compared to the original sample, and no paraffin wax was used.
Therefore, it can be predicted that this sample has a balanced formulation, resulting in proper interaction with the carbon black and compound. Increasing the loading percentage of the nanofiller (carbon quantum dot) in this sample may cause a loss of properties and the formation of system agglomeration.

Table 3. Mechanical result of developed compounds (P-value < 0.05)

Sample	Stress (MPa)	Elongation (%)	Modulus (100%)	Modulus (300%)	Wear (mm^3)
N_1	17.82 ± 1.88	298 ± 25.38	3.54 ± 0.38	5.94 ± 0.52	73 ± 3.18
N_2	16.12 ± 1.47	273 ± 16.68	3.72 ± 0.46	5.90 ± 0.47	76 ± 2.54
N_3	19.92 ± 1.45	306 ± 20.76	4.11 ± 0.42	6.43 ± 0.32	71 ± 4.07
N_4	15.59 ± 1.52	277 ± 16.21	3.36 ± 0.30	5.55 ± 0.61	76 ± 4.17
N_5	12.35 ± 2.44	215 ± 31.85	3.84 ± 0.44	6.10 ± 0.27	82 ± 4.45
Blank Sample	11.10 ± 1.96	279 ± 16.36	2.41 ± 0.39	7.80 ± 0.48	83 ± 2.91

Table 4. Key parameters of TGA analysis of N_3 sample

Sample	$T_{5\%}$ (°C)	T_{max} (°C)	Char Yield(%)
N_3	386.46	553	29.81

5. Conclusion

In general, the compounds containing carbon quantum dot as a substitute for aromatic oil and a part of carbon black did not show a loss of properties in terms of physical, rheological, and thermal properties compared to the commercial blank sample, which can be attributed to the composition and balance impact of nanoparticles in the polymer matrix.
The synthesized carbon quantum dot exhibited a convenient interaction with the rubber compound due to its small size, high surface-to-volume ratio, and carbon-based nature. Additionally, to achieve the specific properties of the elastomeric compound, the effective dispersion of nanoparticles within the polymer matrix plays a crucial role, which is directly related to the amount of nanofiller addition. In other words, when the amount of nanofiller is lower or higher than the proportional limit, it leads to a drop in mechanical and rheological properties. For this reason, in terms of mechanics, the N3 compound presented the highest tensile strength, Modulus, elongation, and the lowest amount of wear compared to other rubber compounds. Finally, from an environmental point of view, the developed carbon quantum dot demonstrates that it could be an appropriate substitute for aromatic oil in the rubber industry due to its acceptable toxicity, low thermal waste, and solubility.

Acknowledgements

We want to thank the Iran Rubber Industry Research Center for their invaluable assistance.

References

[1] Suksaeree J, Pichayakorn W, Monton C, Sakunpak A, Chusut T, Saingam W. Rubber polymers for transdermal drug delivery systems. *Ind Eng Chem Res*. 2014;53(2). doi:10.1021/ie403619b

[2] Schaefer R. Mechanical properties of rubber. In: *Harris' Shock and Vibration Handbook*. ; 2010:6:33-1.

[3] Zhang G, Feng H, Liang K, et al. Design of next-generation cross-linking structure for elastomers toward green process and a real recycling loop. *Sci Bull*. 2020;65(11). doi:10.1016/j.scib.2020.03.008

[4] Basu D, Das A, Stöckelhuber KW, Wagenknecht U, Heinrich G. Advances in layered double hydroxide (LDH)-based elastomer composites. *Prog Polym Sci*. 2014;39(3). doi:10.1016/j.progpolymsci.2013.07.011

[5] Sivaraman R, Roseenid T, Siddanth S. Reinforcement of elastomeric rubber using carbon fiber laminates. *Int J Innov Res Sci Eng Technol*. 2013;2(7):3123-3130.

[6] Yang J, Li K, Tang C, et al. Recent Progress in Double Network Elastomers: One Plus One is Greater Than Two. *Adv Funct Mater*. 2022;32(19). doi:10.1002/adfm.202110244

[7] Jovanović S, Samaržija-Jovanović S, Marković G, Jovanović V, Adamović T, Marinović-Cincović M. Ternary NR/BR/SBR rubber blend nanocomposites. *J Thermoplast Compos Mater*. 2018;31(2). doi:10.1177/0892705717697778

[8] Hwang K, Lee J, Kim W, et al. Comparison of SBR/BR blend compound and ESBR copolymer having same butadiene contents. *Elastomers Compos*. 2019;54(1):54-60.

[9] Wu W, Chen D. Silica-modified SBR/BR blends. *J Appl Polym Sci*. 2011;120(6). doi:10.1002/app.33576

[10] Maurice M. *Rubber Technology*. Springer Science & Business Media; 2013.

[11] Malas A, Pal P, Das CK. Effect of expanded graphite and modified graphite flakes on the physical and thermo-mechanical properties of styrene butadiene rubber/polybutadiene rubber (SBR/BR) blends. *Mater Des*. 2014;55. doi:10.1016/j.matdes.2013.10.038

[12] Gao M, Zheng F, Xu J, et al. Surface modification of nano-sized carbon black for reinforcement of rubber. *Nanotechnol Rev*. 2019;8(1). doi:10.1515/ntrev-2019-0036

[13] Song K, Zhang Y, Meng J, et al. Structural polymer-based carbon nanotube composite fibers: Understanding the processing-structure-performance relationship. *Materials (Basel)*. 2013;6(6). doi:10.3390/ma6062543

[14] Barrera CS, Cornish K. Processing and mechanical properties of natural rubber/waste-derived nano filler composites compared to macro and micro filler composites. *Ind Crops Prod*. 2017;107. doi:10.1016/j.indcrop.2017.05.045

[15] Fan Y, Fowler GD, Zhao M. The past, present and future of carbon black as a rubber reinforcing filler – A review. *J Clean Prod*. 2020;247. doi:10.1016/j.jclepro.2019.119115

[16] Lu Y, Liu J, Hou G, et al. From nano to giant? Designing carbon nanotubes for rubber reinforcement and their applications for high performance tires. *Compos Sci Technol*. 2016;137. doi:10.1016/j.compscitech.2016.10.020

[17] Dwivedi C, Manjare S, Rajan SK. Recycling of waste tire by pyrolysis to recover carbon black: Alternative & environment-friendly reinforcing filler for natural rubber compounds. *Compos Part B Eng*. 2020;200. doi:10.1016/j.compositesb.2020.108346

[18] KUMAR V. Nanofillers in Natural Rubber. *Nat Rubber Mater*. 2013;2: Composi(8):34.

[19] Sahakaro K. Mechanism of reinforcement using nanofillers in rubber nanocomposites. In: *Progress in Rubber Nanocomposites*. ; 2017. doi:10.1016/B978-0-08-100409-8.00003-6

[20] Farshbaf M, Davaran S, Rahimi F, Annabi N, Salehi R, Akbarzadeh A. Carbon quantum dots: recent progresses on synthesis, surface modification and applications. *Artif Cells, Nanomedicine Biotechnol*. 2018;46(7). doi:10.1080/21691401.2017.1377725

[21] Shabbir H, Csapó E, Wojnicki M. Carbon Quantum Dots: The Role of Surface Functional Groups and Proposed Mechanisms for Metal Ion Sensing. *Inorganics*. 2023;11(6). doi:10.3390/inorganics11060262

[22] Kim Y, Jang G, Lee TS. New Fluorescent Metal-Ion Detection Using a Paper-Based Sensor Strip Containing Tethered Rhodamine Carbon Nanodots. *ACS Appl Mater Interfaces*. 2015;7(28). doi:10.1021/acsami.5b04724

[23] Sun Y, Zhang M, Bhandari B, Yang C. Recent Development of Carbon Quantum Dots: Biological Toxicity, Antibacterial Properties and Application in Foods. *Food Rev Int*. 2022;38(7):1513-1532. doi:10.1080/87559129.2020.1818255

[24] Manikandan V, Lee NY. Green synthesis of carbon quantum dots and their environmental applications. *Environ Res*. 2022;212(PB):113283. doi:10.1016/j.envres.2022.113283

[25] Li X, Zhao S, Li B, Yang K, Lan M, Zeng L. Advances and perspectives in carbon dot-based fluorescent probes: Mechanism, and application. *Coord Chem Rev*. 2021;431. doi:10.1016/j.ccr.2020.213686

[26] Gu J, Li X, Zhou Z, et al. 2D MnO 2 nanosheets generated signal transduction with 0D carbon quantum dots: synthesis strategy, dual-mode behavior and glucose detection. *Nanoscale*. 2019;11(27):13058-13068.

[27] Wei JS, Ding C, Zhang P, et al. Robust Negative Electrode Materials Derived from Carbon Dots and Porous Hydrogels for High-Performance Hybrid Supercapacitors. *Adv Mater*. 2019;31(5). doi:10.1002/adma.201806197

[28] Messina MM, Barrionuevo SD, Coustet ME, et al. Graphene and Carbon Dots for Photoanodes with Enhanced Performance. *ACS Appl Nano Mater*. 2021;4(7). doi:10.1021/acsanm.1c01295

[29] Choi Y, Choi Y, Kwon OH, Kim BS. Carbon Dots: Bottom-Up Syntheses, Properties, and Light-Harvesting Applications. *Chem - An Asian J*. 2018;13(6). doi:10.1002/asia.201701736

[30] S. T, D. RS. Green synthesis of highly fluorescent carbon quantum dots from sugarcane bagasse pulp. *Appl Surf Sci*. 2016;390. doi:10.1016/j.apsusc.2016.08.106

[31] Wang Y jing, Zheng G, Shen J, Liu W, Zhu X jun. Simulation of dynamic light scattering signal for ultrafine particles based on the exponential model. *Optoelectron Lett*. 2010;6(4). doi:10.1007/s11801-010-9145-0

[32] Marouzi S, Darroudi M, Hekmat A, Sadri K, Kazemi Oskuee R. One-pot hydrothermal synthesis of carbon quantum dots from Salvia hispanica L. seeds and investigation of their biodistribution, and cytotoxicity effects. *J Environ Chem Eng*. 2021;9(4). doi:10.1016/j.jece.2021.105461

[33] Huang S, Li W, Han P, et al. Carbon quantum dots: Synthesis, properties, and sensing applications as a potential clinical analytical method. *Anal Methods*. 2019;11(17). doi:10.1039/c9ay00068b

[34] Arumugham T, Alagumuthu M, Amimodu RG, Munusamy S, Iyer SK. A sustainable synthesis of green carbon quantum dot (CQD) from Catharanthus roseus (white flowering plant) leaves and investigation of its dual fluorescence responsive behavior in multi-ion detection and biological applications. *Sustain Mater Technol*. 2020;23:e00138. doi:10.1016/j.susmat.2019.e00138

[35] Baweja H, Jeet K. Economical and green synthesis of graphene and carbon quantum dots from agricultural waste. *Mater Res Express*. 2019;6(8). doi:10.1088/2053-1591/ab28e5

[36] Wang RC, Lu JT, Lin YC. High-performance nitrogen doped carbon quantum dots: Facile green synthesis from waste paper and broadband photodetection by coupling with ZnO nanorods.

J Alloys Compd. 2020;813. doi:10.1016/j.jallcom.2019.152201

[37] Vandarkuzhali SAA, Jeyalakshmi V, Sivaraman G, Singaravadivel S, Krishnamurthy KR, Viswanathan B. Highly fluorescent carbon dots from Pseudo-stem of banana plant: Applications as nanosensor and bio-imaging agents. *Sensors Actuators, B Chem*. 2017;252. doi:10.1016/j.snb.2017.06.088

[38] Tang LC, Zhao L, Qiang F, Wu Q, Gong LX, Peng JP. Mechanical properties of rubber nanocomposites containing carbon nanofillers. In: *Carbon-Based Nanofillers and Their Rubber Nanocomposites: Fundamentals and Applications*. ; 2019. doi:10.1016/B978-0-12-817342-8.00012-3

[39] Dhanasekar S, Baskar S, Vishvanathperumal S. Cure characteristics, compression set, swelling behaviors, abrasion resistance and mechanical properties of nanoclay (Cloisite 15A, Cloisite 20A and Cloisite 30B) filler filled EPDM/NBR blend system. *J Polym Res*. 2023;30(10). doi:10.1007/s10965-023-03759-7

[40] Damircheli M, MajidiRad AH. The Influence of the Dispersion Method on the Morphological, Curing, and Mechanical Properties of NR/SBR Reinforced with Nano-Calcium Carbonate. *Polymers (Basel)*. 2023;15(13). doi:10.3390/polym15132963

[41] Poozhikunnath A, Favata J, Ahmadi B, et al. Correlative Microscopy-Based Approach for Analyzing Microscopic Impurities in Carbon Black for Lithium-Ion Battery Applications. *J Electrochem Soc*. 2019;166(14). doi:10.1149/2.0761914jes

[42] Hu Y, Gao Z, Yang J, Chen H, Han L. Environmentally benign conversion of waste polyethylene terephthalate to fluorescent carbon dots for “on-off-on” sensing of ferric and pyrophosphate ions. *J Colloid Interface Sci*. 2019;538. doi:10.1016/j.jcis.2018.12.016

[43] Bhattacharya M, Bhowmick AK. Synergy in carbon black-filled Natural rubber nanocomposites. Part I: Mechanical, dynamic mechanical properties, and morphology. *J Mater Sci*. 2010;45(22). doi:10.1007/s10853-010-4699-6

[44] Song J, Ma L, He Y, Yan H, Wu Z, Li W. Modified graphite filled natural rubber composites with good thermal conductivity. *Chinese J Chem Eng*. 2015;23(5). doi:10.1016/j.cjche.2014.05.022

[45] Sadasivuni KK, Ponnamma D, Thomas S, Grohens Y. Evolution from graphite to graphene elastomer composites. *Prog Polym Sci*. 2014;39(4). doi:10.1016/j.progpolymsci.2013.08.003

[46] Yang J, Tian M, Jia QX, Zhang LQ, Li XL. Influence of graphite particle size and shape on the properties of NBR. *J Appl Polym Sci*. 2006;102(4). doi:10.1002/app.24844

[47] Ismail MN, Khalaf AI. Styrene-butadiene rubber/graphite powder composites: Rheometrical, physicomechanical, and morphological properties. *J Appl Polym Sci*. 2011;120(1). doi:10.1002/app.33101

[48] Saha T, Bhowmick AK. Influence of nanofiller on thermal degradation resistance of hydrogenated nitrile butadiene rubber. *Rubber Chem Technol*. 2019;92(2). doi:10.5254/rct.18.82616

[49] Srivastava SK. Thermal properties of rubber nanocomposites based on carbon nanofillers. In: *Carbon-Based Nanofillers and Their Rubber Nanocomposites: Fundamentals and Applications*. ; 2019. doi:10.1016/B978-0-12-817342-8.00010-X

[50] Farida E, Bukit N, Ginting EM, Bukit BF. The effect of carbon black composition in natural rubber compound. *Case Stud Therm Eng*. 2019;16. doi:10.1016/j.csite.2019.100566

[51]] Namitha LK, Chameswary J, Ananthakumar S, Sebastian MT. Effect of micro- and nano-fillers on the properties of silicone rubber-alumina flexible microwave substrate. *Ceram Int*. 2013;39(6). doi:10.1016/j.ceramint.2013.02.047